ACS APPLIED MATERIALS & INTERFACES

Research Article

www.acsami.org

Carbon Nanotubes Activate Macrophages into a M1/M2 Mixed Status: Recruiting Naïve Macrophages and Supporting Angiogenesis

Jie Meng, Xiaojin Li, Chuan Wang, Hua Guo, Jian Liu, and Haiyan Xu*

Institute of Basic Medical Sciences Chinese Academy of Medical Sciences, School of Basic Medicine Peking Union Medical College, Beijing 100005, P. R. China

Supporting Information

ABSTRACT: The potential of carbon nanotubes (CNTs) in medical applications has been attracting constant research interest as well as raising concerns related to toxicity. The immune system serves as the first line of defense against invasion. In this work, interactions of oxidized multiwalled carbon nanotubes (MWCNT) with macrophages were investigated to unravel the activation profile of macrophages, using cytokine array, ELISA assay, transwell assay, confocal microscopy, and reactive oxygen species examination. Results show that MWCNT initiate phagocytosis of macrophages and upregulate CD14, CD11b, TLR-4/MD2, and CD206, which does not alter the MHCII expression of the macrophages. The macrophages engulfing MWCNT (MWCNT-RAW) secrete a large amount of MIP-1α and MIP-2 to recruit naïve macrophages and produce angiogenesis-related cytokines MMP-9 and VEGF, while inducing much lower levels of proinflammatory cytokines than those activated by LPS. In conclusion, MWCNT activate macrophages into a M1/M2 mixed status, which allows the cells to recruit naïve macrophages and support angiogenesis.

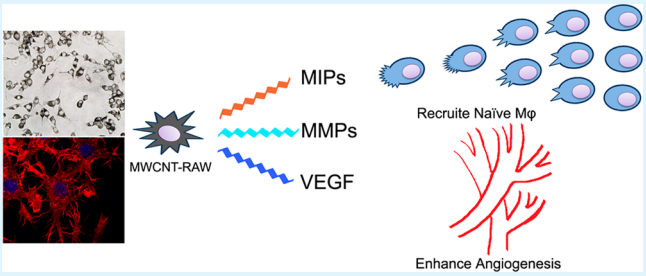

KEYWORDS: *carbon nanotubes, macrophage activation, phenotype, recruitment, angiogenesis*

1. INTRODUCTION

Carbon nanotubes (CNTs) are one of the most attractive nanomaterials in the biomedical and industrial fields because they not only display unique mechanical, chemical, and electrical properties but can be further modified or functionalized with a variety of side-chain moieties.[1−3] These features have made CNTs compelling candidates for the delivery of therapeutic agents and diagnostic probes[4−6] and required rational designs for their application in clinical practice in a safe manner.[7−10] The potential of CNTs in medical applications has been attracting constant research interest as well as raising concerns related to toxicity. The immune system serves as the first line of defense against invasion, being sensitive in the recognition of foreign agents and subsequently regulating the defense response; therefore, an important consideration is the interaction of CNTs with components of the immune system. In the past decade, researchers have made great effort toward a better understanding of CNTs' immunological properties;[11,12] nevertheless, numerous questions are still waiting for clear answers because of the complexity of immune defense mechanisms. Phagocytic cells are the first cellular line of defense of the body, engulfing pathogens and any foreign particulate substances, degrading them, and inducing immune responses. Among the immune effector cells, macrophages are the first phagocytic population encountering CNTs upon intentional administration and occupational exposure. In addition, macrophages have been recognized as one of targeting cells in therapies for inflammation-related diseases such as cancer and atherosclerosis in recent years.[13] For the above reasons, interactions between CNTs and macrophages have been investigated intensely to understand the CNT-mediated behavior of macrophages in depth.

In the literature, CNTs are mainly reported as one toxic stimulus to macrophages, initiating macrophage-based inflammation and resulting in fibrosis formation. For example, CNTs can stimulate macrophages to produce proinflammatory cytokines such as IL-1β, IL-6, INF-γ, TNF-α, etc.,[14,15] through activation of the NF-κb signaling pathway[16−19] or inflammasome formation,[19−23] promoting inflammation and resulting in fibrosis in the lung.[23−27] Nevertheless, some research groups have observed that in some cases CNTs fail to induce strong inflammatory responses.[28−30] For instance, it was reported that CNTs of 220 nm induced lower inflammatory responses than the longer one of 825 nm, and no severe inflammation occurred in the subcutaneous injection model.[29] When mice were intratracheally instilled with a single dose of 60 μg per mouse, only the long multiwalled carbon nanotubes (MWCNT; 5−15 μm) increase collagen deposition and pulmonary fibrosis significantly, while the short MWCNT (350−700 nm) did not.[27] Immunosuppressive effects have also been observed when dendritic cells (DCs) are cultured on MWNT-based films in vitro. The DCs adhering to MWNT films lose polarization

Received: November 2, 2014
Accepted: January 16, 2015
Published: January 16, 2015

DOI: 10.1021/am507649n
ACS Appl. Mater. Interfaces 2015, 7, 3180−3188

ability during maturation to become less efficient in inducing T-cell proliferation with respect to MWCNT−floating DCs and to relevant controls.[31] Our previous study showed that subcutaneously injected MWCNT (average length of about 900 nm) can be taken up by resident macrophages in the injection site with a transient mild inflammatory response, characterized by mild upregulation of proinflammatory cytokines in the serum for 1 week, and only slight fibrosis was observed in the subcutaneous tissue of the injection site.[32]

It has been accepted in recent years that macrophages are plastic and can be activated in different ways and thus take on different functions depending on stimuli received from their microenvironments. Therefore, these conflicting cues imply that macrophage cells may be activated by CNTs with a mixed activation profile, instead of simple proinflammation or immune suppression. To our knowledge, there is little existing literature on the activation signature and associated functions for macrophages upon CNT exposure. In this study, we took oxidized MWCNT with an average length of 900 nm as the model material to explore the effects of CNTs on macrophages' phenotype using cytokine array, ELISA assay, transwell assay, confocal microscopy, and reactive oxygen species (ROS) examination. Our aim is to unravel the distinctive role of CNTs in modulating macrophages' function. We show that MWCNT significantly upregulate recruitment-associated and angiogenesis-associated cytokines, while only inducing mild inflammatory responses much lower than that induced by lipopolysaccharide. The significantly elevated cytokines further recruit naïve macrophages to move toward and internalize MWCNT, forming a positive feedback.

2. MATERIALS AND METHODS

2.1. Preparation and Characterization for MWCNT. MWCNT purchased from Chengdu Organic Chemicals Co. Ltd. were treated and characterized as previously described to be oxidized.[32] In brief, the original MWCNT was suspended in a concentrated H_2SO_4/HNO_3 mixture with the aid of ultrasonication. The mixed solution was neutralized with pure water followed by filtration. The filtered oxidized MWCNT was dried completely and dispersed in a cell culture medium containing 10% heat-inactivated fetal bovine serum (FBS) through sonication (three times, 30 s each; 270 W) in a biological safety hood with a concentration of 1 mg/mL, followed by centrifugation at 1500*g* for 30 min. The supernatant was collected and stored as a stock solution. The concentration of the stock solution was determined by UV−vis−near-IR (NIR) spectroscopy (Lambda 950, PerkinElmer).

2.2. Cell Culture. The mouse macrophage cell line RAW264.7 was purchased from the Cell Bank of Institute of Basic Medical Sciences, Chinese Academy of Medical Sciences, and Peking Union Medical College (Beijing, China). The cells were maintained in Dulbecco's modified Eagle's medium (DMEM) supplemented with 10% heat-inactivated FBS, 4 mM L-glutamine, 4500 mg/L glucose, and 0.1% penicillin G and streptomycin (Invitrogen) at 37 °C with 5% CO_2.

2.3. Cellular Immunostaining and Imaging. Macrophage cells were seeded in a 24-well plate (5×10^4 cells/well); in each well, one coverslip was placed. The cells were incubated overnight to allow adherence. The medium was replaced with 0.5 mL of fresh medium alone or fresh medium containing lipopolysaccharide (LPS; Sigma-Aldrich) at 10 ng/mL or MWCNT at 0.1 mg/mL, followed by 24 h of incubation. Next, the coverslips were rinsed twice with a phosphate-buffered solution (PBS; pH = 7.4). Cells were stained by an actin cytoskeleton kit (Millipore) according to the assay protocol. In brief, the cells were fixed with 4% formaldehyde in PBS for 15 min at room temperature, then washed twice by PBS, and permeabilized in 0.1% Triton X-100 in PBS for 5 min at room temperature. After that, the cells were incubated with the TRITC-conjugated Phalloidin for 1 h at room temperature. Following the wash, nuclei counterstaining was performed by incubating cells with 4′,6-diamidino-2-phenylindole for 5 min at room temperature. The stained cells were subjected to a FluoView FV1000 confocal microscope (Olympus), and images were analyzed using *FluoView* software (Olympus *FLUOVIEW FV 300*, version 3.3).

2.4. Intracellular ROS Measurement. The intracellular ROS of macrophage cells was determined using 2,7-dichlorofluorescin diacetate (DCFH-DA; Sigma) assay. The cells were seeded in 6-well plates (2×10^5 cells/well) and allowed to adhere and proliferate overnight. After that, the medium was replaced with a fresh medium containing MWCNT at 0.03, 0.1, and 0.3 mg/mL or LPS at 10 ng/mL or fresh medium alone for 24 h, followed by washing twice with PBS and further incubation with DCFH-DA at 10 μM at 37 °C for 30 min. Then the cells were washed twice to remove the free DCFH-DA, pipetted, and prepared in a single cell suspension, which was filtered through a filter of 70 μm pore size. The mean fluorescence intensity (MFI) of the cells was determined at 488 nm excitation and 525 nm emission using a flow cytometer (C6, Accuri Cytometers, Ann Arbor, MI) and analyzed using *CFlow* software. The MFI of the samples was divided by that of the control cells, which was indicated as the MFI fold increase of ROS. Data are representative of three independent experiments. The results are presented as mean ± standard deviation (SD).

2.5. Phenotype Assay. Macrophage cells were seeded in 6-well plates at 2×10^5 cells/well and allowed to adhere and proliferate overnight. The cells were then exposed to the medium containing MWCNT at 0.03, 0.1, and 0.3 mg/mL for 24 h. After that, the cells were washed twice with PBS, pipetted, and collected by centrifugation at 1000 rpm for 5 min as a single-cell suspension at a volume of 100 μL. The suspension was incubated with the antibody of FITC-MHCII, FITC-CD14, PE-CD11b, and TLR4/MD-2 complex PE (eBioscience) or the relevant isotypes at 4 °C for 1 h or incubated with primary antibody of CD206 (Biolegend, rat IgG2a), followed by incubation with FITC-labeled antirat IgG (minimal x-reactivity, Biolegend) at 37 °C for 30 min. Next, the cells were washed, filtered, and collected. The fluorescence intensity of the cells was determined using a flow cytometer (C6, Accuri Cytometers, Ann Arbor, MI). The experiment was carried out in duplicate. Data were analyzed using *CFlow* software (Accuri Cytometers). The MFI was presented as the mean ± SD. In order to induce macrophage cells in an alternatively activated state, a combined solution of IL-4, IL-10, and IL-13 (each at 10 ng/mL, ILs-RAW) was added into the cells for 24 h. The expression level of CD206 for ILs−macrophages was also detected using a flow cytometer (C6, Accuri Cytometers, Ann Arbor, MI) and analyzed using *CFlow* software.

2.6. Cytokine Assay. Macrophage cells were incubated with the following medium for 24 h: (1) fresh medium containing LPS at 10 ng/mL, (2) MWCNT at 0.1 mg/mL, (3) a combined solution composed of IL-4, IL-10, and IL-13 (each of 10 ng/mL, termed as ILs), or (4) fresh medium alone, followed by washing twice with PBS. The cells were then lysed using celLytic mammalian cell lysis (Sigma, St. Louis, MO) with protease inhibitor cocktail (Sigma). The lysate was centrifuged at 14000*g* for 15 min at 4 °C. The supernatants were transferred into a clean test tube to quantify the protein concentration using a Pierce BCA protein assay kit (Pierce Biotechnology, Rockford, IL). The cell lysate (0.2 mg) was collected and analyzed for 40 cytokines using mouse cytokine array (R&D system) according to the manufacturer's protocol. Array membranes were analyzed by FluorChem SP multiimaging systems (Alpha Innotech). The average signal (pixel density) of the pair of duplicate spots representing each cytokine was determined by using *FluoChem* software (version 6.0.0). The relative changes of signals on different arrays were compared between samples treated by MWCNT or LPS or ILs and the control.

2.7. Western Blot Analysis for MIP-1α and MIP-2 in a Culture Medium. Macrophage cells were incubated with a MWCNT at 0.1 mg/mL for 4, 12, and 24 h. Supernatants of 1 mL were collected at each time point and freeze dried. A total of 100 μL of distilled water was added to each sample. An equal volume of the supernatant (30 μL) was loaded and separated on 12% polyacrylamide gels (Applygen, Beijing, China) and transferred to poly(vinylidene difluoride)

DOI: 10.1021/am507649n
ACS Appl. Mater. Interfaces 2015, 7, 3180−3188

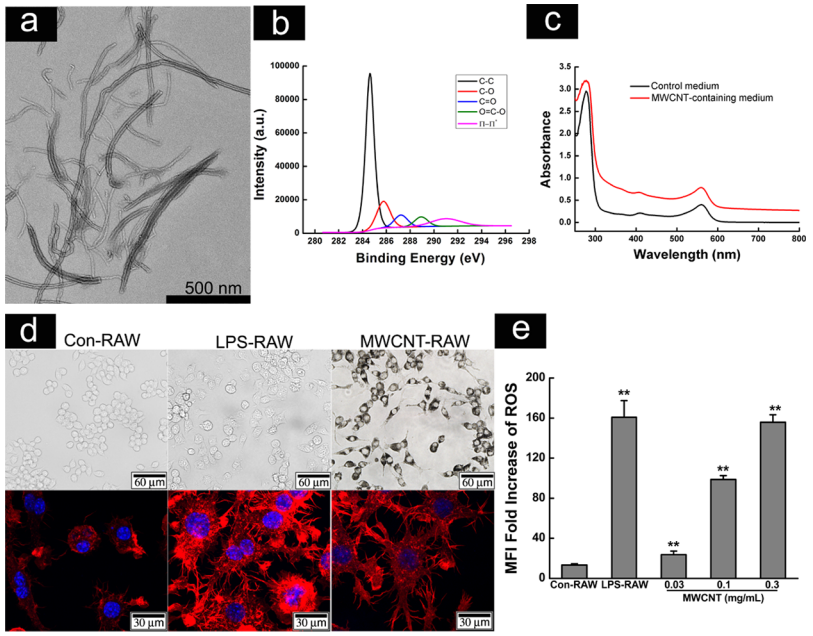

Figure 1. MWCNT initiate macrophages phagocytosis: (A) TEM image of MWCNT. (B) XPS spectrum of MWCNT. (C) UV−vis−NIR spectrum of MWCNT dispersed in the cell culture medium. (D) Microscopic and confocal images of Con-RAW, LPS-RAW, and MWCNT-RAW. The cells were stained with actin (red) and nuclei (blue). (E) ROS production of LPS-RAW and MWCNT-RAW with three concentrations: (**) $p < 0.01$ and (*) $p < 0.05$ versus Con-RAW. Data shown are representative of the results of three individual experiments.

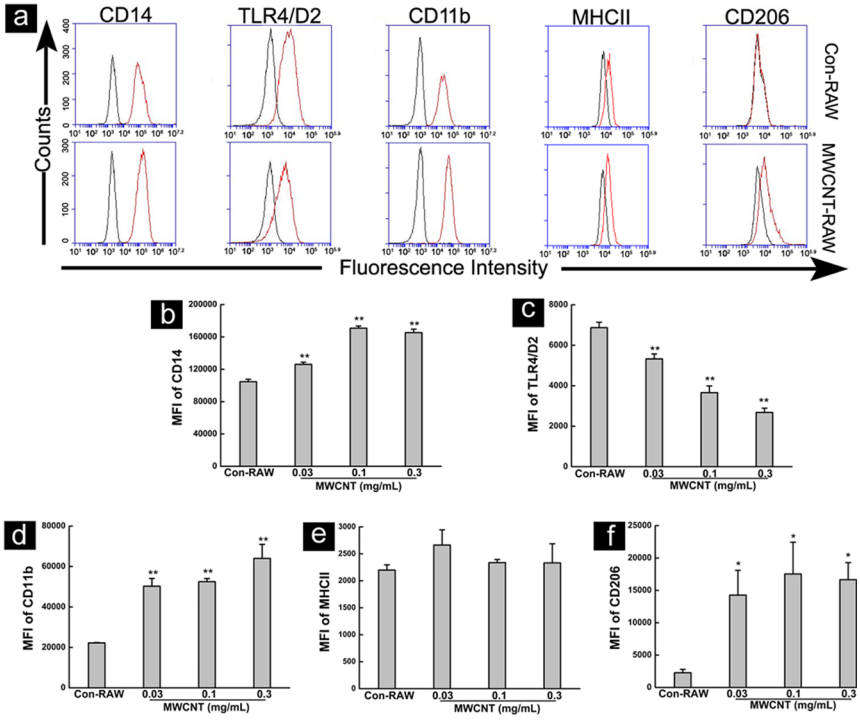

Figure 2. Flow cytometry analysis of macrophage surface marker expression: (A) Representative histogram showing fluorescence of CD14, TLR4/MD2, CD11b, MHCII, and CD206 on the surface of macrophages in the presence or absence of MWCNT. The isotype control is presented as a black line. (B−F) MFI of CD14, TLR4/MD2, CD11b, MHCII, and CD206 on the macrophages treated with 0.03, 0.1, and 0.3 mg/mL MWCNT, respectively: (**) $p < 0.01$ and (*) $p < 0.05$ vs Con-RAW. Data shown are representative of the results of three individual experiments.

membranes (0.45 μm; Millipore, Bedford, MA). The macrophage inflammation protein-1α (MIP-1α), macrophage inflammation protein-2 (MIP-2), and β-actin were probed with specific primary antibodies (anti-Murine MIP-1α, R&D; anti-Murine MIP-2, Peprotech; anti-β-Actin, Cell Signaling Technology, Beverly, MA) and secondary antibodies conjugated to horseradish peroxidase (HRP; Zhongshan Golden Bridge Biotechnology Co., Beijing, China). The immunocomplex on the membrane was visualized using Image Quant LAS 4000 (GE Healthcare) with a HRP Substrate luminol reagent and peroxide solution (Millipore, Billerica, MA). Macrophage cells cultured in a normal cell medium were processed by the same procedure and served as the control.

2.8. MMP-9 and VEGF Examination. Macrophage cells treated with MWCNT at 0.03, 0.1, and 0.3 mg/mL, respectively. After 24 h of

DOI: 10.1021/am507649n
ACS Appl. Mater. Interfaces 2015, 7, 3180−3188

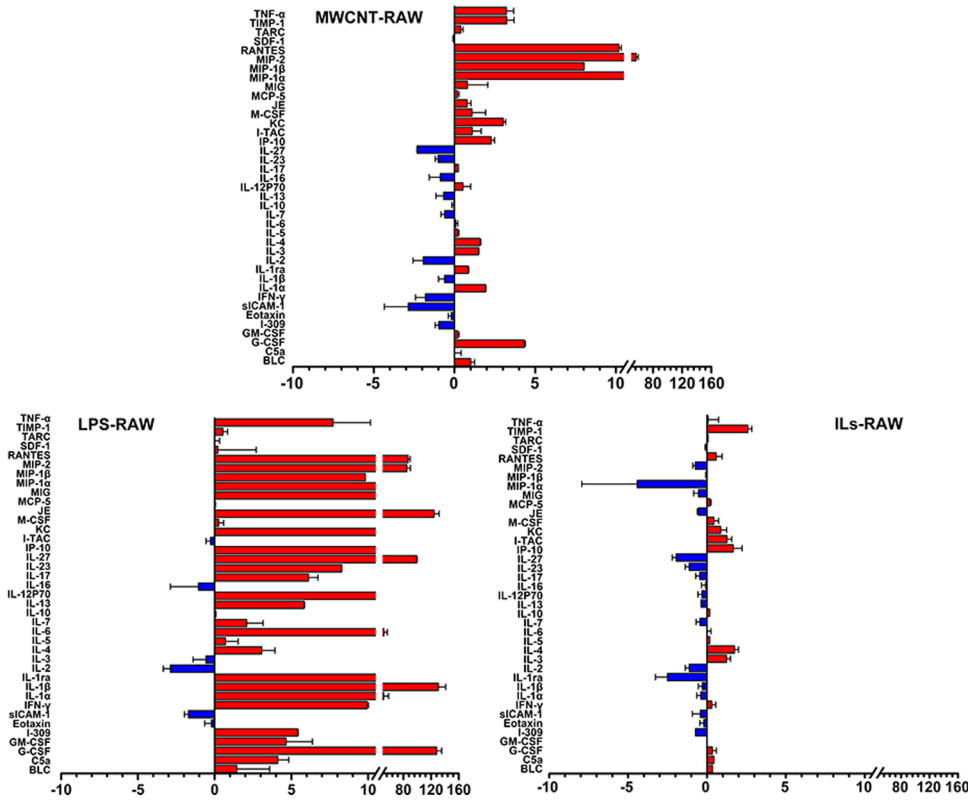

Figure 3. Relative proinflammatory cytokine expression of LPS-RAW, MWCNT-RAW, and ILs-RAW. The relative variation of signals on different arrays is compared between samples treated by MWCNT or LPS or ILs and Con-RAW. Data shown are representative of the results of two individual experiments.

incubation, culture media were collected and centrifuged at 14000*g* for 15 min. The supernatant was transferred to a clean test tube and used to assess the matrix metallopeptidase 9 (MMP-9) and vascular endothelial growth factor (VEGF) concentrations using the mouse MMP-9 and VEGF ELISA kits (R&D), respectively, following the manufacturer's instructions. The absorbance at 450 nm was measured and transferred into the concentrations of MMP-9 and VEGF according to the calibration curve. The experiment was carried out in duplicate. Data were expressed as the mean ± SD.

2.9. Transwell Assay. *MWCNT-Recruited Migration.* Macrophage cells were added in the hanging cell culture insert (1×10^5 cells/well) of the transwell device. A total of 800 μL of the MWCNT-containing cell culture medium was added in the lower chamber at 0.1 mg/mL. After incubation for designated times (4, 12, and 24 h), macrophage cells on the upper surface of the insert were carefully removed by wiping with a cotton swab. Cells on the bottom of the inset were fixed with 4% paraformaldehyde in PBS, washed, then stained with 0.1% crystal violet for 1 h, and subjected to an inverted microscope (Olympus IX71). The absorbance of eluted crystal violet at a wavelength of 570 nm was measured using a BioTek Synergy 4 Hybrid Multi-Mode Microplate Reader (BioTek Instruments, Winooski, VT) and converted to the viable cell number through a linear calibration curve. The experiments shown are representative of three independent experiments. To examine the concentration effect, three doses of MWCNT of 0.03, 0.1, and 0.3 mg/mL were added to the lower chamber, and macrophage cells in the hanging insert were incubated for 24 h. The migrating cells were counted as described above.

Neutralization of MIP-1α, MIP-2, and MMP-9. The antibody of MIP-1α (R&D) or MIP-2 (Peprotech) was supplemented in the lower chamber at 1 μg/mL. The MMPs inhibitor Batimastat (BB-94, Celleck Chemicals) was added into the lower chamber at 4 or 8 nM. The inhibition percentage of cell migration was determined using the same protocol as that mentioned above.

2.10. Statistics. Statistical analysis was performed using Microsoft Excel (Microsoft Software 2007). Data were analyzed by a two-tailed Student's *t* test for paired samples. Differences were considered to be significant for $p < 0.05$.

3. RESULTS

3.1. MWCNT Initiate Macrophage Cell Phagocytosis and Activation. MWCNT used in this study have length distributions from 500 nm to 2 μm; the average value is about 900 nm, counted statistically from 10 transmission electron microscopy (TEM) images (Figure 1a). Various oxygen-containing groups were detected on the surface of MWCNT, including C−O (286 eV), C═O (287 eV), and O═C−OH (289 eV) appearing in the X-ray photoelectron spectrometry (XPS) spectrum (Figure 1b). MWCNT were able to be dispersed well in the cell culture medium for at least 2 weeks without changing the characteristic UV−vis−NIR spectrum of the culture medium (Figure 1c).

When macrophage cells were incubated with a MWCNT-containing culture medium, phagocytosis was initiated. The cells engulfed large amounts of MWCNT, which made the cellular plasma become black (Figure 1d, upper panel), while the cell body became larger (MWCNT-RAW). Phagocytosis is a cytoskeleton-dependent process, leading to cell morphology changes. It can be seen that naïve macrophages (con-RAW) displayed transparent cytoplasm without filopoda; the F-actin (red fluorescence) mainly diffused into the cytoplasm; LPS-treated macrophages (LPS-RAW) displayed F-actin distribution throughout all of the cells; differently, the F-actin was compacted in the elongated filopoda and around the nucleus of MWCNT-RAW, suggesting that MWCNT-RAW had a different activation status from that induced by LPS.

DOI: 10.1021/am507649n
ACS Appl. Mater. Interfaces 2015, 7, 3180−3188

Table 1. Relative Mean Pixel Density of LPS-RAW, MWCNT-RAW, and ILs-RAW

	LPS	MWCNT	ILs
BLC	1.44 ± 2.14	1.00 ± 0.24	0.34 ± 0.00
C5a	4.11 ± 0.72	0.01 ± 0.41	0.43 ± 0.00
G-CSF	128.04 ± 7.27	4.32 ± 0.08[a,b]	0.34 ± 0.25
GM-CSF	4.65 ± 1.72	0.19 ± 0.09[a]	0.002 ± 0.00
I-309	5.42 ± 0.02	−0.98 ± 0.23[a]	−0.74 ± 0.00
Eotaxin	−0.21 ± 0.44	−0.21 ± 0.18[a]	−0.20 ± 0.25
sICAM-1	−1.71 ± 0.26	−2.87 ± 1.48	−0.43 ± 0.51
IFN-γ	9.93 ± 0.09	−1.80 ± 0.62[a,b]	0.30 ± 0.25
IL-1α	51.20 ± 7.48	1.92 ± 0.03[a,b]	−0.40 ± 0.25
IL-1β	130.57 ± 10.53	−0.62 ± 0.38[a]	−0.30 ± 0.25
IL-1ra	12.52 ± 3.42	0.85 ± 0.03[a]	−2.51 ± 0.76
IL-2	−2.89 ± 0.46	−1.94 ± 0.63	−1.13 ± 0.25
IL-3	−0.56 ± 0.85	1.49 ± 0.03[a]	1.23 ± 0.25
IL-4	3.07 ± 0.86	1.57 ± 0.06	1.74 ± 0.25
IL-5	0.70 ± 0.83	0.20 ± 0.08	0.17 ± 0.00
IL-6	51.74 ± 5.04	0.09 ± 0.12[a]	0 ± 0.25
IL-7	2.08 ± 1.07	−0.61 ± 0.23	−0.45 ± 0.25
IL-10	0.04 ± 0.04	−0.04 ± 0.12	0.17 ± 0.00
IL-13	5.82 ± 0.04	−0.67 ± 0.48[a]	−0.38 ± 0.00
IL-12P70	10.58 ± 1.83	0.52 ± 0.48[a]	−0.32 ± 0.25
IL-16	−1.05 ± 1.83	−0.88 ± 0.68	−0.09 ± 0.25
IL-17	6.12 ± 0.61	0.24 ± 0.01[a]	−0.47 ± 0.25
IL-23	8.28 ± 4.39	−1.01 ± 0.18	−1.14 ± 0.25
IL-27	99.20 ± 0.74	−2.32 ± 0.02[a]	−1.95 ± 0.25
IP-10	35.75 ± 1.75	2.27 ± 0.21[a]	1.66 ± 0.56
I-TAC	−0.27 ± 0.29	1.10 ± 0.56	1.26 ± 0.31
KC	39.78 ± 0.98	3.02 ± 0.15[a,b]	0.86 ± 0.38
M-CSF	0.26 ± 0.33	1.08 ± 0.84	0.43 ± 0.31
JE	124.33 ± 7.31	0.78 ± 0.24[a,b]	−0.55 ± 0.08
MCP-5	0.02 ± 0.04	0.18 ± 0.11	0.18 ± 0.08
MIG	35.49 ± 5.26	0.80 ± 1.27	−0.55 ± 0.31
MIP-1α	21.34 ± 12.83	40.22 ± 2.99[a,b]	−4.43 ± 3.51
MIP-1β	9.82 ± 1.48	8.03 ± 2.87	−0.04 ± 0.05
MIP-2	84.99 ± 5.17	56.84 ± 2.87[a,b]	−0.75 ± 0.15
RANTES	87.02 ± 2.90	10.18 ± 0.15[a,b]	0.58 ± 0.38
SDF-1	0.20 ± 2.51	−0.05 ± 0.05	−0.05 ± 0.08
TARC	0.02 ± 0.31	0.38 ± 0.15[a]	0.07 ± 0.00
TIMP-1	0.54 ± 0.31	3.23 ± 0.45[a]	2.58 ± 0.25
TNF-α	7.72 ± 2.43	3.22 ± 0.45[a,b]	0.07 ± 0.66
TREM-1	5.08 ± 1.33	−0.59 ± 0.45[a]	0.29 ± 0.20

[a] $p < 0.05$ between the MWCNT and LPS groups. [b] $p < 0.05$ between the MWCNT and ILs groups.

Phagocytosis of macrophages requires extra respiration, and the "respiratory burst" turned out to the formation of ROS.[33] We further examined the ROS level of macrophages induced by MWCNT exposure. It was clearly shown that LPS violently stimulated ROS generation in macrophages, with about a 12-fold increase of the MFI in reference to the control level. MWCNT exposure resulted in ROS production too, which was concentration-dependent. When the concentration of MWCNT was 0.03 mg/mL, ROS induction was a 2-fold increase of the MFI compared to the control. As the concentration was increased to 0.1 mg/mL, there was a 8-fold increase of the MFI. MWCNT at 0.3 mg/mL induced the highest ROS production, which is comparable to LPS at 10 ng/mL.

3.2. Effects of MWCNT on the Phenotype of Macrophages. Macrophages can show an activation spectrum depending on what stimulating signals they receive from the environment. M1 and M2 represent the two extremes in the activation spectrum: M1 macrophages promote inflammatory reactions and antitumoral responses, while M2 macrophages regulate immunological responses and enhance wound healing.[34] We asked whether MWCNT induced macrophages of a specific activation signature and examined the cell surface markers of MWCNT-RAW. The polyspecific receptor (CD14), a complex of tolllike receptor 4 and myeloid differentiation factor 2 (TLR4/MD2), CD11b, mannose receptor (MR, or named as CD206), and the main histocompatible complex II (MHCII) were selected and measured through flow cytometry (Figure 2).

CD14 is expressed predominantly on the surface of monocytes and macrophages, presenting an invading substance to the complex of TLR4/MD2 and further signaling inside the cell. It was shown that MWCNT upregulated the CD14 level significantly, while it downregulated the TLR4/MD2 level in a concentration-dependent manner. When cells coexpress CD14 and TLR4, CD14 expression promotes TLR4 endocytosis;[35] it is reasonable to suggest that MWCNT induces TLR4 endocytosis, which results in the downregulation of TLR4/MD2. CD11b is a pattern recognition receptor, capable of recognizing and binding to many molecules found on the surface of invading bacteria or foreign cells. MWCNT induced a concentration-dependent rising level of CD11b, indicating that phagocytosis of macrophages was initiated. In phagocytosis, foreign substances or antigens are processed into peptides in the cell and delivered to the surface of the cell with major histocompatible complex class II (MHCII), facilitating antigen presentation. However, the level of MHC II was not upregulated by MWCNT, even at the highest concentration of 0.3 mg/mL in the current study. To the contrary of MHCII, CD206, one of the markers indicating alternative activation for macrophages,[36,37] was elevated significantly by MWCNT. Taken altogether, MWCNT were internalized largely by macrophages and activated macrophages in a specific way that is different either from the classical activation way or from the alternative activation way. This result implies that macrophage cells do not take MWCNT as dangerous exogenous antigens.

3.3. MWCNT Induced a Different Profile of Proinflammatory Cytokines. In order to further figure out the activation status for macrophage cells upon MWCNT exposure, we examined the function of cytokine secretion using a protein array for 40 kinds of proinflammatory cytokine (R&D). In this assay, LPS was taken as a classical activation stimulus, and a combination of IL4, IL10, and IL13 (ILs) was used to induce macrophages in the alternative activation.[38] As shown in Figure 3 and Table 1, macrophages were activated classically by LPS, an most of the proinflammatory cytokines were significantly upregulated. On the contrary, macrophages did not produce significant proinflammatory cytokines upon IL treatment. Differently, many of the proinflammatory cytokines were not increased significantly by MWCNT in reference to those by LPS. For examples taken from Table 1, typical proinflammatory cytokines such as IL-1α, IL-1β, IL-6, IL-12p70, IL-17, TNF-α, MCP-1, G-CSF, GM-CSF, and C5a were elevated little upon MWCNT exposure. However, it is noticeable that macrophage inflammatory protein-1 alpha (MIP-1α) and MIP-2 and tissue inhibitor of metalloproteinases 1 (TIMP-1) were upregulated significantly by MWCNT: MIP-1α was twice that induced by LPS, MIP-2 was at a comparable level with that induced by

DOI: 10.1021/am507649n
ACS Appl. Mater. Interfaces 2015, 7, 3180−3188

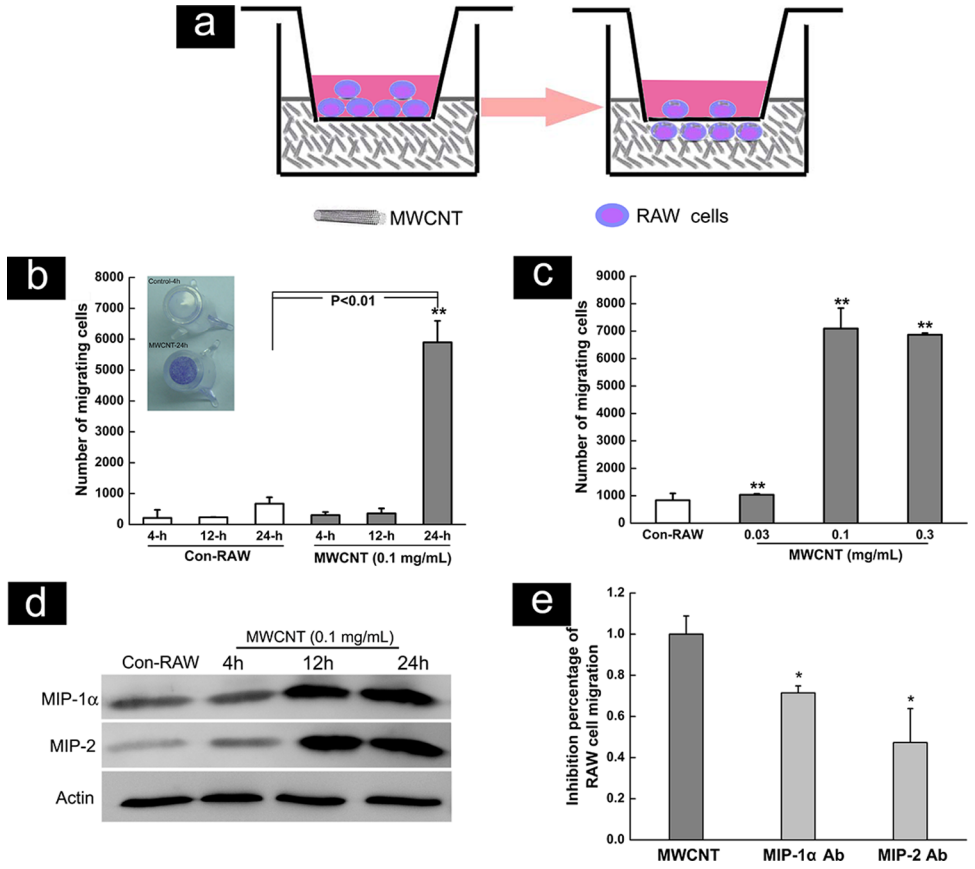

Figure 4. Macrophage migration induced by MIP-1α and MIP-2 produced by macrophages encountered with MWCNT: (A) Schematic graph. (B) Macrophage migration in a time-dependent manner. The inset figure is a representative image of transwell inserts: (**) $p < 0.01$ vs Con-RAW 4 h. (C) MWCNT-concentration-dependent recruitment of macrophage: (**) $p < 0.01$ vs Con-RAW. (D) Western blot results showing that MWCNT-RAW induces an incubation time elevation in MIP-1α and MIP-2 production. (E) Recruitment of macrophage neutralized by MIP-1α and MIP-2 specific antibodies, respectively: (*) $p < 0.05$ vs MWCNT as the control. Data shown are representative of the results of three individual experiments.

LPS, and TIMP-1 was about 6 times that induced by LPS. The signature of MWCNT-mediated macrophage activation is clearly different from that of LPS- or IL-mediated activation.

3.4. MWCNT Initiate the Recruitment Function of Macrophage Cells. Both MIP-1α and MIP-2 belong to a superfamily of small proteins with the typical function of recruiting macrophages and lymphocytes. Therefore, we assume that MWCNT-RAW may act as a core producing recruiting-related cytokines to attract naïve macrophages. The transwell assay was applied to verify whether MWCNT initiates the recruitment function of macrophages. As illustrated in the schematic Figure 4a, naïve macrophages were added in the upper chamber and a MWCNT-containing cell culture medium was added in the bottom chamber. It was seen that, after 24 h of incubation, a large number of macrophages migrated into the lower chamber, while little migrated into the control medium (Figure 4b). It is noticeable that the migration is strongly dependent on the incubation time; no obvious cell migration was observed until 12 h of incubation. The effect of MWCNT to initiate the recruitment function of macrophages is also associated with the concentration of MWCNT. The number of migrated cells was increased dramatically when the concentration of MWCNT was increased from 0.03 to 0.1 mg/mL; however, no further promotion was observed when the concentration of MWCNT was increased to 0.3 mg/mL (Figure 4c). We consider that 0.3 mg/mL MWCNT induced the cytotoxicity slightly (Figure S1 in the Supporting Information), and the cell viability was about 80% of the control, which makes some of migrating cells lose their ability to secrete cytokines and attract more naïve macrophages.

In order to understand the time effect of the recruitment function for MWCNT, Western blot assay was applied to examine the production of MIP-1α and MIP-2 for macrophages incubated with MWCNT in different times. Results show that MWCNT-RAW exhibited an incubation time-dependent elevation in MIP-1α and MIP-2 production. As shown in Figure 4d, macrophages did not produce significant amount of MIP-1α until 12 h incubation with MWCNT, and synthesized the highest amount of MIP-1α after 24 h incubation. The production of MIP-2 displayed similar time-course pattern to that of MIP-1α, which reached the plateau of high expression after 12 h incubation. The neutralization assay was performed by supplementing the antibody of MIP-1α or MIP-2 in the MWCNT-containing culture medium in the lower chamber. The supplemented antibody of MIP-1α inhibited 30% of the migration of macrophage cells and the supplemented antibody of MIP-2 inhibited 50% of the migration (Figure 4e). According to these results we infer that macrophages simultaneously migrating into the lower chamber engulf MWCNT in the culture medium and produce recruiting-related cytokines subsequently. It is time-consuming to accumulate cytokines including MIP-1α and MIP-2 enough

DOI: 10.1021/am507649n
ACS Appl. Mater. Interfaces 2015, 7, 3180−3188

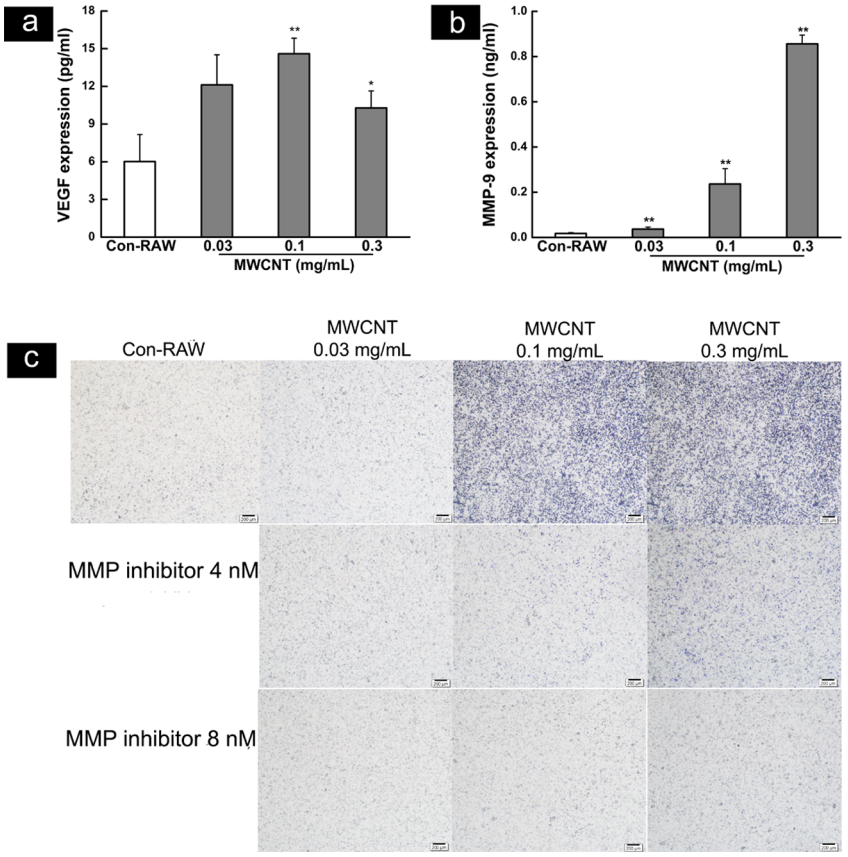

Figure 5. MWCNT inducing macrophage cells to secrete VEGF (A) and MMP-9 (B). (C) Representative microscopic images of the transwell inserts of macrophages encountered with MWCNT and MMP inhibitors. First row: Images of macrophages migration when the MWCNT concentration is 0.03, 0.1, and 0.3 mg/mL in the bottom chamber; MMP inhibitor of 4 nM (second row) and 8 nM (third row) inhibiting MWCNT-mediated macrophage migration: (*) $p < 0.05$ and (**) $p < 0.01$ vs Con-RAW. Data shown are representative of the results of three individual experiments.

to attract naïve macrophages in the upper chamber to migrate into the lower chamber.

3.5. MWCNT Induce Macrophage Cells To Secrete Repair-Related MMP9 and VEGF. The results that MWCNT-RAW exhibits a constant level of MHCII and an elevated level of CD206 and produces a high amount of TIMP-1 imply that MWCNT-RAW may act like alternatively activated macrophages (M2) supporting tissue repair. M2 macrophages secrete a variety of matrix metalloproteins (MMPs) to promote the fusion of blood vessels, especially highly inducible MMP-9 and VEGF.[38] Hence, we next examined the secretion of MMP-9 and VEGF for MWCNT-RAW. Results show that MWCNT-RAW secreted MMP-9 (Figure 5a) and VEGF (Figure 5b) depending on the concentration of MWCNT. It is known that the activity of MMP-9 is regulated by its endogenous inhibitor TIMP-1. It has been reported that the synthesis of MMP-9 and TIMP-1 under control of the same transcription factors, MMP-9 and TIMP-1, forms a balance to control the physiological process including migration, angiogenesis, and wound healing.[39] In the current study, MWCNT-RAW significantly produced not only TIMP-1 but also MMP-9, which may guarantee MWCNT-RAW in a balanced function of tissue degradation and formation.

In the wound-healing process, MMP-9 and VEGF also play recruitment roles for macrophage cells. Here we took MMP-9 as an example to verify the recruitment function of MWCNT-RAW resulting from MMP-9 secretion. In the transwell assay (Figure 5c), when the MMP inhibitor Batimastat was supplemented in a MWCNT-containing cell culture medium in the lower chamber at 0.4 nM, the migration of macrophage cells mediated by MWCNT at 0.1 mg/mL was inhibited significantly, while 8 nM Batimastat stopped the migration of macrophage cells induced by MWCNT at 0.3 mg/mL.

4. DISCUSSION

Macrophages are prodigious phagocytic cells that are involved in the removal of cellular debris that is generated during tissue remodeling and rapidly and efficiently clear cells that have undergone apoptosis. These processes result in little or no production of immune mediators by unstimulated macrophages. On the contrary, phagocytosis of necrosis that results from trauma or stress by macrophages leads to dramatic changes in their physiology, including alterations in the expression of surface proteins and the production of cytokines and proinflammatory mediators, because the debris from necrosis is usually loaded with endogenous danger signals.[34]

Activated by LPS or a combination of IL4/IL-10/IL-13 (ILs), macrophages displayed distinctive contrary statuses. When treated by LPS, macrophages were classically activated, secreting a large amount of proinflammatory cytokines including IL-1β, IFN-γ, and TNF-α, with significantly elevated MHC-II levels. However, ILs-RAW displayed a totally different cytokine expressing profile, with very low proinflammatory cytokines and elevated CD206, indicating its activation status of

DOI: 10.1021/am507649n
ACS Appl. Mater. Interfaces 2015, 7, 3180−3188

M2. Compared with the profile of proinflammatory cytokines induced by LPS, the most apparent change was that MWCNT-RAW secreted larger amounts of MIP-1α and MIP-2 than LPS-RAW, which resulted in the dramatic migration of naïve macrophage cells toward to MWCNT-RAW. These attracted cells would take up MWCNT and produce MIP-1α and MIP-2 too, which allowed MIP-1α and MIP-2 to accumulate constantly to form a feedback loop of recruiting naïve macrophages. Therefore, MWCNT-RAW can act as a core of attracting naïve macrophage cells but not a source inducing severe inflammations. We previously reported that subcutaneously injected MWCNT constantly recruited blood-derived monocyte/macrophage cells in the mouse breast cancer tumor model, however, did not induce significant inflammation in the subcutaneous tissue around the administration site.[40] One group reported that CNTs induced moderate cell infiltration and cytokine production (TNF-α and IL-β), which was much lower than that of LPS, while the concentration of MIP-1α in BAL fluid significantly increased by about 32.2-fold at 24 h after instillation of 4 mg/kg single-walled CNT compared to the vehicle control.[41] These results are consistent with the observation in the current study.

As for MWCNT-RAW, it is also interesting that the level of MHCII was kept constant; meanwhile, most of the proinflammatory cytokines in the array were mildly upregulated except for several recruitment-related cytokines, suggesting that macrophages do not regard MWCNT as a hazard like LPS. Meanwhile, the CD206 level was elevated significantly, along with secretion of MMP-9 and VEGF. Both MMP-9 and VEGF are closely associated with wound healing through the promotion of angiogenesis. From these data emerge the following results: (1) MWCNT-RAW is partially activated in the classical way and partially in the alternative way, showing a CNT-mediated specific activation signature. (2) MWCNT-RAW has double faces; it combines functions of M1 and M2. It plays the M1 function to secrete recruiting-related cytokines to recruit naïve macrophages and the M2 function to produce MMP-9 and VEGF, which are potent in angiogenesis.

5. CONCLUSIONS

MWCNT initiates phagocytosis of macrophages and upregulates CD14, CD11b, TLR-4/MD2, and CD206 and does not alter MHCII expression of the macrophages. MWCNT-RAW secretes a large amount of MIP-1α and MIP-2 to recruit naïve macrophages while producing angiogenesis-related cytokines MMP-9 and VEGF. MWCNT-RAW induces much lower levels of proinflammatory cytokines than LPS-RAW, indicating that MWCNT does not induce classical inflammatory responses in macrophages. Taken altogether, MWCNT activates macrophages into a M1/M2 mixed status, which allows the macrophages to have the functions of recruiting naïve macrophages and supporting angiogenesis.

■ ASSOCIATED CONTENT

Supporting Information

Viability of cells incubated with MWCNT at different concentrations evaluated using a CCK-8 agent. This material is available free of charge via the Internet at http://pubs.acs.org.

■ AUTHOR INFORMATION

Corresponding Author

*E-mail: xuhy@pumc.edu.cn.

Notes

The authors declare no competing financial interest.

■ ACKNOWLEDGMENTS

The authors are thankful for financial support from the National Key Program of China (973 Program 2011CB933504) and the National Natural Science Foundation of China (Grant 81000665).

■ REFERENCES

(1) Foldvari, M.; Bagonluri, M. Carbon Nanotubes as Functional Excipients for Nanomedicines: I. Pharmaceutical Properties. *Nanomedicine* **2008**, *4*, 173−182.
(2) Battigelli, A.; Ménard-Moyon, C.; Da Ros, T.; Prato, M.; Bianco, A. Endowing Carbon Nanotubes with Biological and Biomedical Properties by Chemical Modifications. *Adv. Drug Delivery Rev.* **2013**, *65*, 1899−1920.
(3) Zhang, Y.; Bai, Y.; Yan, B. Functionalized Carbon Nanotubes for Potential Medicinal Applications. *Drug Discovery Today* **2010**, *15*, 428−435.
(4) Foldvari, M.; Bagonluri, M. Carbon Nanotubes as Functional Excipients for Nanomedicines: II. Drug Delivery and Biocompatibility Issues. *Nanomedicine* **2008**, *4*, 183−200.
(5) Wong, B. S.; Yoong, S. L.; Jagusiak, A.; Panczyk, T.; Ho, H. K.; Ang, W. H.; Pastorin, G. Carbon Nanotubes for Delivery of Small Molecule Drugs. *Adv. Drug Delivery Rev.* **2013**, *65*, 1964−2015.
(6) Bates, K.; Kostarelos, K. Carbon Nanotubes as Vectors for Gene Therapy: past Achievements, Present Challenges and Future Goals. *Adv. Drug Delivery Rev.* **2013**, *65*, 2023−33.
(7) Beg, S.; Rizwan, M.; Sheikh, A. M.; Hasnain, M. S.; Anwer, K.; Kohli, K. Advancement in Carbon Nanotubes: Basics, Biomedical Applications and Toxicity. *J. Pharm. Pharmacol.* **2011**, *63*, 141−163.
(8) Stern, S. T.; McNeil, S. E. Nanotechnology Safety Concerns Revisited. *Toxicol. Sci.* **2008**, *101*, 4−21.
(9) Shvedova, A. A.; Kisin, E. R.; Porter, D.; Schulte, P.; Kagan, V. E.; Fadeel, B.; Castranova, V. Mechanisms of Pulmonary Toxicity and Medical Applications of Carbon Nanotubes: Two Faces of Janus? *Int. Encycl. Pharmacol. Ther.* **2009**, *121*, 192−204.
(10) Lanone, S.; Andujar, P.; Kermanizadeh, A.; Boczkowski, J. Determinants of Carbon Nanotube Toxicity. *Adv. Drug Delivery Rev.* **2013**, *65*, 2063−2069.
(11) Dobrovolskaia, M. A.; McNeil, S. E. Immunological Properties of Engineered Nanomaterials. *Nat. Nanotechnol.* **2007**, *2*, 469−478.
(12) Orecchioni, M.; Bedognetti, D.; Sgarrella, F.; Marincola, F. M.; Bianco, A.; Delogu, L. G. Impact of Carbon Nanotubes and Graphene on Immune Cells. *J. Transl. Med.* **2014**, *12*, 138.
(13) Wynn, T. A.; Chawla, A.; Pollard, J. W. Macrophage Biology in Development, Homeostasis and Disease. *Nature* **2013**, *496*, 445−455.
(14) Sun, Z.; Liu, Z.; Meng, J.; Meng, J.; Duan, J.; Xie, S.; Lu, X.; Zhu, Z.; Wang, C.; Chen, S.; Xu, H.; Yang, X. D. Carbon Nanotubes Enhance Cytotoxicity Mediated by Human Lymphocytes in vitro. *PLoS One* **2011**, *6*, e21073.
(15) Qu, C.; Wang, L.; He, J.; Tan, J.; Liu, W.; Zhang, S.; Zhang, C.; Wang, Z.; Jiao, S.; Liu, S.; Jiang, G. Carbon Nanotubes Provoke Inflammation by Inducing the Pro-inflammatory Genes IL-1β and IL-6. *Gene* **2012**, *493*, 9−12.
(16) Manna, S. K.; Sarkar, S.; Barr, J.; Wise, K.; Barrera, E. V.; Jejelowo, O.; Rice-Ficht, A. C.; Ramesh, G. T. Single-walled Carbon Nanotube Induces Oxidative Stress and Activates Nuclear Transcription Factor-kappaB in Human Keratinocytes. *Nano Lett.* **2005**, *5*, 1676−84.
(17) He, X.; Young, S. H.; Schwegler-Berry, D.; Chisholm, W. P.; Fernback, J. E.; Ma, Q. Multiwalled Carbon Nanotubes Induce a Fibrogenic Response by Stimulating Reactive Oxygen Species Production, Activating NF-κB Signaling, and Promoting Fibroblast-to-Myofibroblast Transformation. *Chem. Res. Toxicol.* **2011**, *24*, 2237−2248.

DOI: 10.1021/am507649n
ACS Appl. Mater. Interfaces 2015, 7, 3180−3188

(18) Gao, N.; Zhang, Q.; Mu, Q.; Bai, Y.; Li, L.; Zhou, H.; Butch, E. R.; Powell, T. B.; Snyder, S. E.; Jiang, G.; Yan, B. Steering Carbon Nanotubes to Scavenger Receptor Recognition by Nanotube Surface Chemistry Modification Partially Alleviates NFκB Activation and Reduces its Immunotoxicity. *ACS Nano* **2011**, *5*, 4581−4591.
(19) Hamilton, R. F., Jr.; Wu, Z.; Mitra, S.; Shaw, P. K.; Holian, A. Effect of MWCNT Size, Carboxylation, and Purification on in vitro and in vivo Toxicity, Inflammation and Lung Pathology. *Part. Fibre Toxicol.* **2013**, *10*, 57.
(20) Palomäki, J.; Välimäki, E.; Sund, J.; Vippola, M.; Clausen, P. A.; Jensen, K. A.; Savolainen, K.; Matikainen, S.; Alenius, H. Long, Needle-like Carbon Nanotubes and Asbestos Activate the NLRP3 Inflammasome Through a Similar Mechanism. *ACS Nano* **2011**, *5*, 6861−6870.
(21) Yang, M.; Flavin, K.; Kopf, I.; Radics, G.; Hearnden, C. H.; McManus, G. J.; Moran, B.; Villalta-Cerdas, A.; Echegoyen, L. A.; Giordani, S.; Lavelle, E. C. Functionalization of Carbon Nanoparticles Modulates Inflammatory Cell Recruitment and NLRP3 Inflammasome Activation. *Small* **2013**, *9*, 4194−4206.
(22) Hamilton, R. F., Jr.; Buford, M.; Xiang, C.; Wu, N.; Holian, A. NLRP3 Inflammasome Activation in Murine Alveolar Macrophages and Related Lung Pathology is Associated with MWCNT Nickel Contamination. *Inhalation Toxicol.* **2012**, *24*, 995−1008.
(23) Hussain, S.; Sangtian, S.; Anderson, S. M.; Snyder, R. J.; Marshburn, J. D.; Rice, A. B.; Bonner, J. C.; Garantziotis, S. Inflammasome Activation in Airway Eepithelial Cells after Multi-walled Carbon Nanotube Exposure Mediates a Profibrotic Response in Lung Fibroblasts. *Part. Fibre Toxicol.* **2014**, *11*, 28.
(24) Muller, J.; Huaux, F.; Moreau, N.; Misson, P.; Heilier, J. F.; Delos, M.; Arras, M.; Fonseca, A.; Nagy, J. B.; Lison, D. Respiratory Toxicity of Multi-wall Carbon Nanotubes. *Toxicol. Appl. Pharmacol.* **2005**, *207*, 221−231.
(25) Porter, D. W.; Hubbs, A. F.; Mercer, R. R.; Wu, N.; Wolfarth, M. G.; Sriram, K.; Leonard, S.; Battelli, L.; Schwegler-Berry, D.; Friend, S.; Andrew, M.; Chen, B. T.; Tsuruoka, S.; Endo, M.; Castranova, V. Mouse Pulmonary Dose- and Time Course-responses Induced by Exposure to Multi-walled Carbon Nanotubes. *Toxicology* **2010**, *269*, 136−147.
(26) Morimoto, Y.; Horie, M.; Kobayashi, N.; Shinohara, N.; Shimada, M. Inhalation Toxicity Assessment of Carbon-based Nanoparticles. *Acc. Chem. Res.* **2013**, *46*, 770−781.
(27) Chen, T.; Nie, H.; Gao, X.; Yang, J.; Pu, J.; Chen, Z.; Cui, X.; Wang, Y.; Wang, H.; Jia, G. Epithelial−mesenchymal Transition Involved in Pulmonary Fibrosis Induced by Multi-walled Carbon Nanotubes via TGF-beta/Smad Signaling Pathway. *Toxicol. Lett.* **2014**, *226*, 150−162.
(28) Shvedova, A. A.; Kisin, E. R.; Mercer, R.; Murray, A. R.; Johnson, V. J.; Potapovich, A. I.; Tyurina, Y. Y.; Gorelik, O.; Arepalli, S.; Schwegler-Berry, D.; Hubbs, A. F.; Antonini, J.; Evans, D. E.; Ku, B. K.; Ramsey, D.; Maynard, A.; Kagan, V. E.; Castranova, V.; Baron, P. Unusual Inflammatory and Fibrogenic Pulmonary Responses to Single-walled Carbon Nanotubes in Mice. *Am. J. Physiol. Lung Cell Mol. Physiol.* **2005**, *289*, L698−708.
(29) Sato, Y.; Yokoyama, A.; Shibata, K.; Akimoto, Y.; Ogino, S.; Nodasaka, Y.; Kohgo, T.; Tamura, K.; Akasaka, T.; Uo, M.; Motomiya, K.; Jeyadevan, B.; Ishiguro, M.; Hatakeyama, R.; Watari, F.; Tohji, K. Influence of Length on Cytotoxicity of Multi-walled Carbon Nanotubes Against Human Acute Monocytic Leukemia Cell Line THP-1 in vitro and Subcutaneous Tissue of Rats in vivo. *Mol. BioSyst.* **2005**, *1*, 176−182.
(30) Bellucci, S.; Chiaretti, M.; Cucina, A.; Carru, G. A.; Chiaretti, A. I. Multiwalled Carbon Nanotube Buckypaper: Toxicology and Biological Effects in vitro and in vivo. *Nanomedicine (London, U.K.)* **2009**, *4*, 531−540.
(31) Aldinucci, A.; Turco, A.; Biagioli, T.; Toma, F. M.; Bani, D.; Guasti, D.; Manuelli, C.; Rizzetto, L.; Cavalieri, D.; Massacesi, L.; Mello, T.; Scaini, D.; Bianco, A.; Ballerini, L.; Prato, M.; Ballerini, C. Carbon Nanotube Scaffolds Instruct Human Dendritic Cells: Modulating Immune Responses by Contacts at the Nanoscale. *Nano Lett.* **2013**, *13*, 6098−6105.
(32) Meng, J.; Yang, M.; Jia, F.; Xu, Z.; Kong, H.; Xu, H. Immune Responses of BALB/c Mice to Subcutaneously Injected Multi-walled Carbon Nanotubes. *Nanotoxicology* **2011**, *5*, 583−591.
(33) Dupré-Crochet, S.; Erard, M.; Nüβe, O. ROS Production in Phagocytes: Why, When, and Where? *J. Leukocyte Biol.* **2013**, *94*, 657−670.
(34) Mosser, D. M.; Edwards, J. P. Exploring the Full Spectrum of Macrophage Activation. *Nat. Rev. Immunol.* **2008**, *8*, 958−969.
(35) Zanoni, I.; Ostuni, R.; Marek, L. R.; Barresi, S.; Barbalat, R.; Barton, G. M.; Granucci, F.; Kagan, J. C. CD14 Controls the LPS-induced Endocytosis of Toll-like Receptor 4. *Cell* **2011**, *147*, 868−880.
(36) Mills, C. D.; Kincaid, K.; Alt, J. M.; Heilman, M. J.; Hill, A. M. M-1/M-2 Macrophages and the Th1/Th2 Paradigm. *J. Immunol.* **2000**, *164*, 6166−6173.
(37) Luo, Y.; Zhou, H.; Krueger, J.; Kaplan, C.; Lee, S. H.; Dolman, C.; Markowitz, D.; Wu, W.; Liu, C.; Reisfeld, R. A.; Xiang, R. Targeting Tumor-associated Macrophages as a Novel Strategy Against Breast Cancer. *J. Clin. Invest.* **2006**, *116*, 2132−2141.
(38) Mehra, N. K.; Mishra, V.; Jain, N. K. A Review of Ligand Tethered Surface Engineered Carbon Nanotubes. *Biomaterials* **2014**, *35*, 1267−1283.
(39) Hassan, F.; Ren, D.; Zhang, W.; Gu, X. X. Role of c-Jun N-terminal Protein Kinase 1/2(JNK1/2) in Macrophage-mediated MMP-9 Production in Response to Moraxella Catarrhalis Lipooligosaccharide (LOS). *PLoS One* **2012**, *7*, e37912.
(40) Yang, M.; Meng, J.; Cheng, X.; Lei, J.; Guo, H.; Zhang, W.; Kong, H.; Xu, H. Multiwalled Carbon Nanotubes Interact with Macrophages and Influence Tumor Progression and Metastasis. *Theranostics* **2012**, *2*, 258−270.
(41) Inoue, K.; Takano, H.; Koike, E.; Yanagisawa, R.; Sakurai, M.; Tasaka, S.; Ishizaka, A.; Shimada, A. Effects of Pulmonary Exposure to Carbon Nanotubes on Lung and Systemic Inflammation with Coagulatory Disturbance Induced by Lipopolysaccharide in Mice. *Exp. Biol. Med. (Maywood)* **2008**, *233*, 1583−1590.

DOI: 10.1021/am507649n
ACS Appl. Mater. Interfaces 2015, 7, 3180−3188